UDC 57.087:577.352.5

Estimation of Multiple Cardiac Cells' Action Potentials From Extracellular Field Potentials

Shpotak M. O., Ivanushkina N. H., Ivanko K. O., Prokopenko Y. V.

National Technical University of Ukraine "Igor Sikorsky Kyiv Polytechnic Institute", Kyiv, Ukraine

E-mail: *mykhailo.shpotak@gmail.com*

Modern biomedical technologies use a combination of microelectrode array (MEA) systems and artificially grown cells to study disease mechanisms and test drug effects. MEA systems measure extracellular field potentials (FPs) of cell cultures or tissues, but they cannot record intracellular action potentials (APs) without some modifications or additional devices, limiting the depth of electrophysiological analysis. One of the possible solutions to the inability of MEA systems to measure APs is to mathematically reconstruct them using recorded FPs. However, accurately reconstructing APs of multiple cells is challenging task, which is complicated by many factors such as the number of cells, synchronicity of their APs, identification of their electrophysiological parameters, and noise. This paper aims to address the mathematical problem of AP synchronicity, asynchronicity and partial synchronicity between multiple cells. In this study, mathematical techniques were employed to derive a system of equations capable of reconstructing the APs of N cells simultaneously, using the FPs recorded with $N+1$ electrodes. The equations take into account the number of cells, synchronicity and variation of their APs and specific electrical properties of the cells and the medium. In numerical experiments the equations were applied to reconstruct APs from FPs for cases with different types of synchronicity in noise-free and noisy conditions. The reconstructed APs, when combined with recorded FPs, expand the number of electrophysiological characteristics available for cardiotoxicity assessment in MEA systems.

Keywords: action potentials; field potentials; signal reconstruction; signal synchronicity; numerical modelling; cellular electrophysiology; microelectrode array

DOI: 10.20535/RADAP.2023.93.70-77

Introduction

In the pharmaceutical field micro-electrode array (MEA) systems are used to measure field potentials (FPs) of different human or animal cells exposed to therapeutic agents [1]. Specifically, in cardiac field researchers use MEA systems with different types of cardiac cells to study the effects of antiarrhythmic drugs [2]. Depending on the cardiac cell type, FP (and action potential (AP)) recordings have different signal morphology, duration and amplitude [3]. There are cardiac cells that cannot generate AP (and FP) without external electrical stimulation and the cardiac cells that can, such as the sinoatrial node (SAN) cells, which are called cardiac pacemakers because they are capable of spontaneously generating APs [4]. Understanding how a drug affects the potentials generated by the cardiac cells allows to assess the drug's antiarrhythmic properties and make predictions about its effect on heart rhythm. While MEA is used for measuring FPs, patch-clamp is widely used method for recording the AP. The downside of patch-clamp is a need to interact with a cell membrane by capturing an ion channel. Such direct interaction allows measuring cell's transmembrane current and voltage, so that the researcher can assess cell's electrophysiological characteristics. Conducting comparative studies about AP and FP by analysing the correlation between their temporal characteristics allows researchers to make conclusions about cardiotoxicity based on both AP and FP [5]. There is a number of methods available to measure both AP and FP at the same time, but all of them have their strengths and drawbacks. Some MEA systems are manufactured with nanotube electrodes which can penetrate the cell membrane to measure the intracellular APs [6–8], but this also can result in damage of varying degrees to the cell membrane [9]. The different approach to MEA is the usage of opto- or electroporation systems which can alter permeability of the membrane and allow recording the intracellular potentials without physically penetrating the membrane [10–13]; the drawback of this method is that it may cause cell damage as a result of phototoxicity [14]. As an alternative to the technological methods of simultaneous AP/FP measuring, the biophysical relationship between AP and FP can be mathematically modelled to reconstruct AP from FP [15]. In combination with MEA systems, this approach offers a

non-invasive way to monitor the APs of excitable cells such as neurons and cardiac cells, utilizing electrodes in the extracellular environment to avoid cellular damage. Understanding cardiac cells behaviour is essential to cardiotoxicity research, but using only FP recordings to analyse their activity can be limiting. By reconstructing APs and quantifying characteristics like amplitude and duration, the effect of pharmacological compounds on the cell culture can be assessed more effectively.

1 Problem statement

Reconstruction of APs from the recorded FPs introduces a variety of challenges. The method proposed in [15] is intended for synchronous electrical activity, it can be used under the assumption that all cells exhibit identical and synchronous AP morphology. However, this approach falters when diverse AP generation frequencies lead to varied signal morphologies or when the AP propagation results in time-delayed signals. In these situations, relying solely on a synchronicity-based reconstruction approach becomes untenable.

As an example of asynchronicity in AP generation, Fig. 1a shows a frame from the video recording of a contracting cardiac tissue in μECG device introduced in [16]. μECG allows tracking the electrical activity in lab-grown cardiac tissues. Unlike MEA which uses stationary electrodes, μECG uses a micro-electrode channel guide technology, which allows to safely insert and position 3D wire-shaped probes in specific areas of the cardiac tissue to record its FPs. Figure 1b shows a segmented video frame with colours representing dominant contraction frequencies of the respective regions. In this case, dominant frequency of the FP matched the dominant contraction frequency of the tissue. Regions with other contraction frequencies had no evident effect on the FP recording. Unlike μECG device, which has the electrodes on the sides and the middle of the 10 mm long tissue channel (resulting in approximately 5 mm or 10 mm electrode spacing), MEA systems typically have much smaller electrode spacing of around 0.3 mm (300 μm) [12], therefore the effects of asynchronous AP could be more prevalent.

2 Research objectives

The primary goal of this paper is to adapt the AP reconstruction technique proposed in [15] for the scenario when multiple cells exhibit asynchronous or partially synchronous behaviours. Specifically, the simulation of time-delayed AP asynchronicity is presented to demonstrate how applying the method intended for synchronous cell behaviour in asynchronous scenarios can affect the AP characteristics.

3 Methods

In [15] the formula for reconstructing the AP of a cardiac cell from their FP was proposed. The reconstruction method is based on the idea of treating a cell as a point sources of current, whose electrical field can be observed as FP at some reasonable distance away from the cell. Combining the formulas of the model of parallel conductances and the electric field of a point charge resulted in equation for a single cell and two electrodes:

$$\varphi_2 - \varphi_1 = \frac{C_m}{4\pi\sigma}\frac{\partial u_m}{\partial t}\left(\frac{1}{r_1} - \frac{1}{r_2}\right), \tag{1}$$

where φ_1 and φ_2 are extracellular potentials recorded from the first and second electrodes, respectively; r_1 and r_2 is distance from the current source to the first and second electrodes, respectively; C_m is the cell membrane capacitance; σ is the specific conductivity of the extracellular medium; u_m is the potential of the cell membrane.

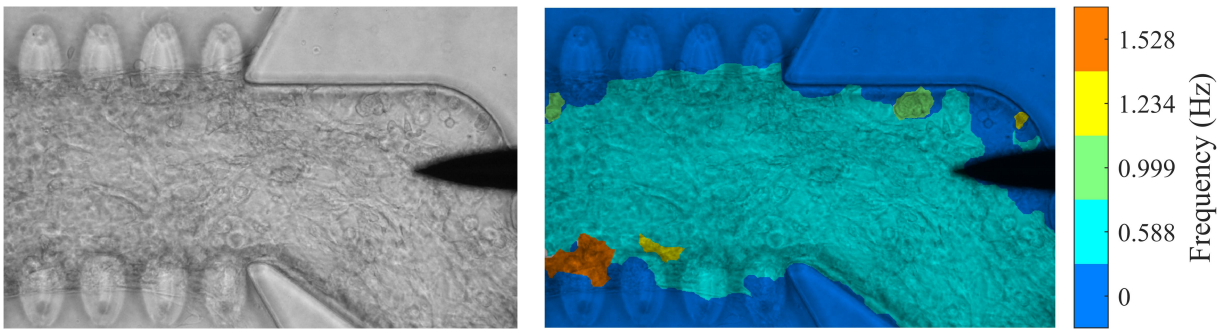

(a) (b)

Fig. 1. A frame from the video of a cultured cardiac tissue contracting in μECG device (a), with its frequency-based segmentation overlay (b) where different colours represent dominant contracting frequencies

Integrating equation (1) resulted in the formula, which shows the relationship between AP u_m and FP difference $\varphi_2 - \varphi_1$:

$$u_m(t) = u_0 + \frac{4\pi\sigma}{C_m\left(\frac{1}{r_1} - \frac{1}{r_2}\right)} \int_0^t (\varphi_2 - \varphi_1)\, dt, \quad (2)$$

where u_0 is the membrane potential at the time $t = 0$.

A case with one cell and two electrodes is described by formula (2). However, MEA systems are typically used together with cell cultures instead of a singular cell, so the cases with multiple cells have to be considered. In the case of N cells and 2 electrodes the next formula can be used [15]:

$$u_m(t) = \\ = u_0 + \frac{4\pi\sigma}{\sum_{i=1}^{N} C_{mi}\left(\frac{1}{r_{i1}} - \frac{1}{r_{i2}}\right)} \int_0^t (\varphi_2 - \varphi_1)\, dt. \quad (3)$$

The FP of each cell is recorded by M electrodes, resulting in $M - 1$ equations:

$$\varphi_{j+1} - \varphi_j = \\ = \frac{C_m}{4\pi\sigma}\frac{du_m}{dt}\left(\frac{1}{r_j} - \frac{1}{r_{j+1}}\right), \quad j = \overline{1, M-1}. \quad (4)$$

A potential at any point of space is equal to the sum of potentials from all surrounding sources:

$$\varphi_1 = \sum_{i=1}^{N} \varphi_{i1}, \qquad \varphi_2 = \sum_{i=1}^{N} \varphi_{i2}, \quad (5)$$

where φ_{i1} and φ_{i2} are potentials induced by a source i on the electrode 1 and 2 respectively.

$$\varphi_2 - \varphi_1 = \frac{C_m}{4\pi\sigma}\frac{du_m}{dt}\sum_{i=1}^{N}\left(\frac{1}{r_{i1}} - \frac{1}{r_{i2}}\right). \quad (6)$$

In the formula (6) all cells are synchronised in generating the identical membrane potential, thus resulting in a single unknown variable um. In case of non-identical APs or asynchronous potential generation, the number of unknown variables grows corresponding to the number of cells N $(u_{m1}, u_{m2}, \ldots, u_{mN})$, which makes it impossible to reconstruct all the APs using only one equation. A case for N cells and M electrodes consists of N by $M - 1$ equations from (4). A system of equations for a cell i and M electrodes can be described by:

$$\varphi_{i,j+1} - \varphi_{i,j} = \\ = \frac{C_m}{4\pi\sigma}\frac{du_{mi}}{dt}\left(\frac{1}{r_{i,j}} - \frac{1}{r_{i,j+1}}\right), \quad j = \overline{1, M-1}. \quad (7)$$

Applying formulas (5) to equation (7) gives a system of $M - 1$ equations with N unknown variables:

$$\sum_{i=1}^{N}\left(\left(\frac{1}{r_{i,j}} - \frac{1}{r_{i,j+1}}\right)(u_{mi}(t) - u_{0i})\right) = \\ = \frac{4\pi\sigma}{C_m}\int_0^t (\varphi_{j+1} - \varphi_j)\, dt, \quad j = \overline{1, M-1}. \quad (8)$$

In order to solve system of equations (8) the number of electrodes M has to be bigger than the number of cells N by 1. If the APs are identical and synchronous, then APs of multiple cells can be treated as a single AP, so $u_{mi}(t) - u_{0i}$ becomes $u_m(t) - u_0$ and equation (8) can be presented as follows:

$$(u_m(t) - u_0)\sum_{i=1}^{N}\left(\frac{1}{r_{i,j}} - \frac{1}{r_{i,j+1}}\right) = \\ = \frac{4\pi\sigma}{C_m}\int_0^t (\varphi_{j+1} - \varphi_j)\, dt, \quad j = \overline{1, M-1}. \quad (9)$$

The initial AP values u_{0i} and u_0 are usually unknown for equations (8) and (9) respectively, but they can be determined by comparing the difference $u_m(t) - u_0$ at distinct parts of the reconstructed AP with a modelled or measured AP values of the cell type used in the experiment (e.g. the resting potential and the maximum amplitude at the peak of the AP).

The membrane capacitance C_m is different for each cell because of the multitude of factors such as cell geometry, genetic variation, epigenetic modifications, etc., but a possible modelling simplification is to assume C_m to be the same for all cells of the same type.

Since the MEA systems are designed to measure FPs, the distances between the cells and the electrodes are unknown, so in order to solve equations (8) or (9) all the r_{ji} have to be identified. In formula (3) (and similarly in equation (9)) the sum of differences of inverse distances can be moved to the right side of the equation to be expressed as a part coefficient before the integral; that way its identification becomes a matter of correct scaling. In equation (8) there are multiple u_{mi}, so resolving the equation requires the identification of $2N$ distances for $M - 1$ equations and the coefficient scaling has to be done for each $u_{mi}(t) - u_{0i}$.

In addition to the cases of synchronous and asynchronous behaviour there can also be partial synchronicity. In case of synchronicity all cells in the area generate APs simultaneously, which results in the synchronized FPs that can be measured by the electrodes; in the asynchronous case there is a delay in APs the cells generate, which results in the asynchronous FPs; partial synchronicity can occur when some cells are synchronous while others are not. For example, if there are two groups of cells and each group has identical but asynchronous APs, then equation (8) can be replaced with equation (9) partially, effectively reducing the number of equations by the number of cells with synchronous AP.

4 Results

Demonstrating the reconstruction of APs from FPs for the cases of asynchronicity and synchronicity requires a two-dimensional numerical experiment involving multiple cells and electrodes. First, an improved parallel conductance model from [17] was used to simulate the human sinoatrial node (SAN) APs for multiple cells. Then, their FPs were determined on the basis of field theory. Lastly, to reconstruct APs from FPs, the system of equations (8) was used; the integral terms in the system were approximated using cumulative trapezoidal numerical integration, adhering to the uniform step size set by the 2 kHz sampling frequency of the signals.

Table 1 Positions of cells and electrodes

	Cell position			Electrode position			
Point	C_1	C_2	C_3	E_1	E_2	E_3	E_4
x, μm	200	450	500	300	300	600	600
y, μm	300	600	650	600	300	600	300

Table 2 Initial sinoatrial node AP model values

Case	Sync		Async		Partial sync		
Cell	C_1	C_2	C_1	C_2	C_1	C_2	C_3
u_0, mV	-50	-50	-50	-60	-50	-60	-60
Whole-cell capacitance, pF	56.6 [18]						
Medium conductivity, S/m	1.5 [19]						

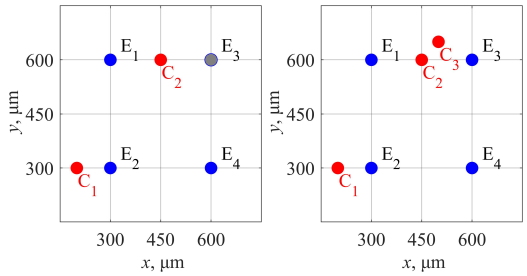

Fig. 2. The maps of the cell and electrode positions: (a) 2 cells with 3 active electrodes (and 1 inactive); (b) 3 cell with 4 active electrodes

Both cases of synchronicity and asynchronicity need at least 2 cells and 3 electrodes to be simulated. Figure 2a and Table 1 show the cell and electrode positions. The electrodes were arranged into a grid pattern to resemble the MEA system electrodes.

In order to present the AP reconstruction in both noiseless and denoised scenarios for a more comprehensive view, Gaussian white noise with a mean of 0 and standard deviation of 2.3 μV was independently generated for each FP. Additionally, power-line interference, consisting of a fundamental frequency of 50 Hz at an amplitude of 10 μV, and its associated harmonics were added to the FPs; the amplitudes of the harmonics were attenuated according to an inverse proportional decay, expressed as $1/k$, where k denotes number of the harmonic. Finally, to minimize noise, the signals were processed using a comb filter and wavelet denoising [15].

In the case of AP synchronicity all the cells are assumed to be generate the same AP. This means that APs of any number of cells can be treated as a simple 1 AP case and solved with one of the equations from (9), which requires the FPs from any 2 electrodes to be known. If the cells have non-identical yet synchronous AP, then using (9) will result in a weighted average depending on the distances from the cell to the electrodes (unless the coefficients before the integral are different).

For the synchronous case, the cell AP model parameters were selected to be the same for both cells C_1 and C_2 (Table 2), resulting in 2 identical and synchronous APs. Figure 3d,e shows the 2 APs reconstructed from the FPs in Fig. 3a-c. The red APs are identical because they were reconstructed from the noiseless FPs, while the black APs differ because they were reconstructed from the imperfectly denoised FPs.

The asynchronous case requires solving the system of equations (8). The reconstructed asynchronous AP are shown in Fig. 4. Table 2 shows the initial parameters of the cell model; using a different initial potential for the second AP preserves its morphology, but introduces a time delay, resulting in asynchronicity between two APs.

A possible simplification for the asynchronous case is to consider some of the APs to be synchronous, which defines a case of partial synchronicity. In asynchronous approach reconstructing APs from 3 cells would require FPs from at least 4 electrodes, but if 2 cells have synchronous and identical APs and 1 cell has a different or/and asynchronous AP, then all the APs can be reconstructed with only 3 electrodes.

Map on the Fig. 2b shows an additional cell C_3 placed close to the cell C_2 and an additional active electrode E_3. Table 2 shows that synchronous cells have different initial potentials than the asynchronous cell, resulting in time delay between 2 groups of cells. The reconstructed APs for the case of partial synchronicity are shown in Fig. 5; blue AP potentials are synchronized with each other, while the red AP is asynchronous with the blue APs because of the time delay.

5 Discussion

According to the results of the numerical experiment the APs can be reconstructed from the FPs if the number of cells is smaller than the number of electrodes. If the number of unknown APs is bigger than the number of equations, then the system of equations can't be solved without some simplifications like complete or partial synchronicity.

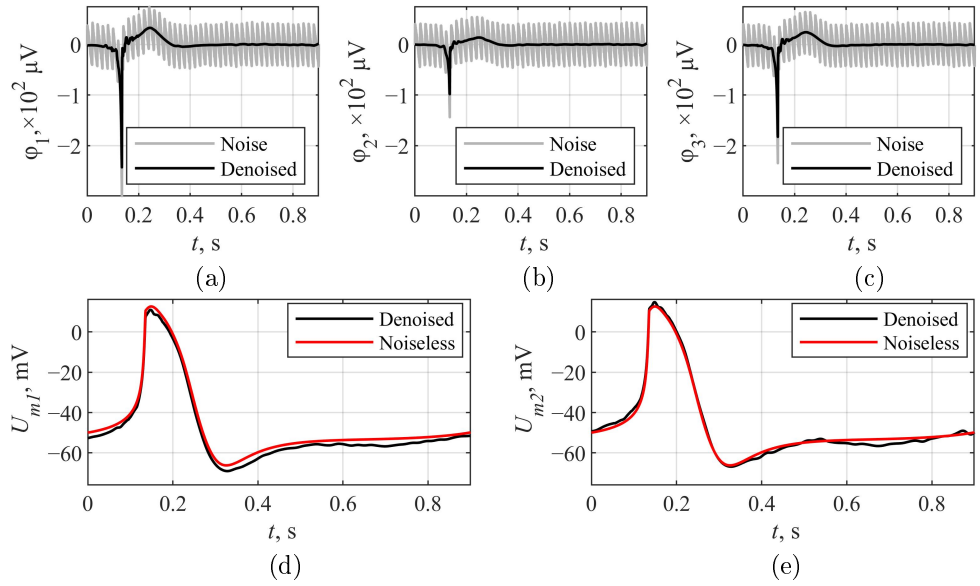

Fig. 3. Reconstruction of synchronous APs. Top figures (a, b, c) show the FPs, simulated to represent recordings from the respective electrodes; bottom figures show the APs of the cells C_1 (d) and C_2 (e), reconstructed from the noiseless and denoised FPs (black and red)

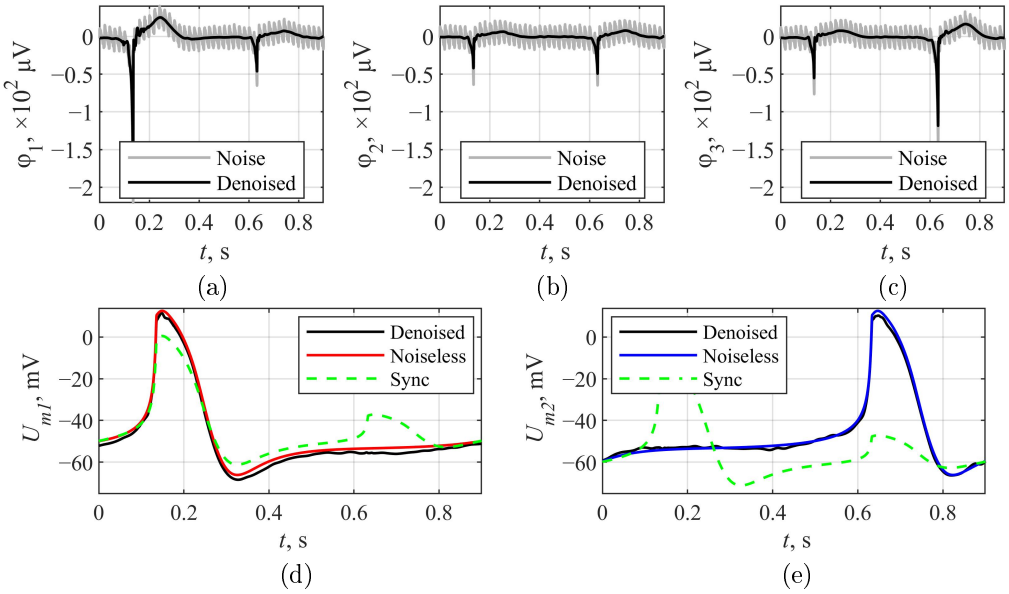

Fig. 4. Reconstruction of asynchronous APs. Top figures (a, b, c) show the FPs, simulated to represent recordings from the respective electrodes; bottom figures show the APs of the cells C_1 (d) and C_2 (e), reconstructed from the noiseless and denoised FPs using equation (8) for asynchronous approach (black, red and blue) and the APs reconstructed from noiseless FP using equation (9) for synchronous approach (green)

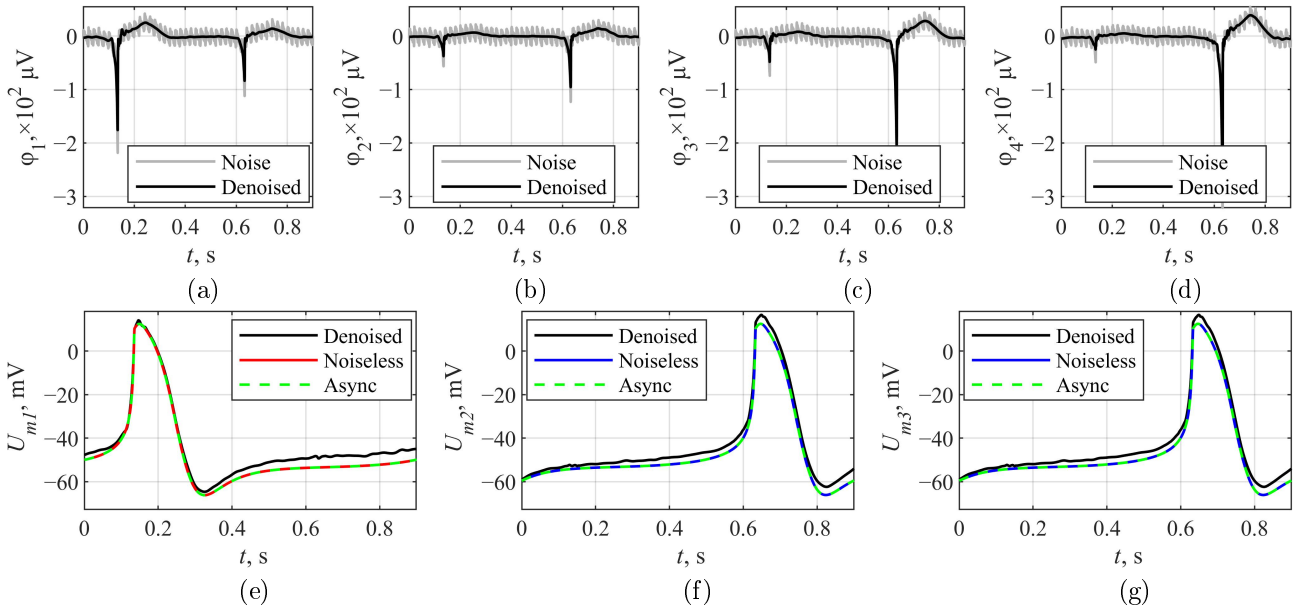

Fig. 5. Reconstruction of partially synchronous APs. Top figures (a, b, c, d) show the FPs, simulated to represent recordings from the respective electrodes; bottom figures show the AP of the cells C_1 (e), C_2(f) and C_3 (g), reconstructed from the noiseless and denoised FPs under the assumption of partial synchronicity (black, red and blue) using only 3 electrodes and the APs reconstructed from noiseless FP under the assumption of asynchronicity (green) using 4 electrodes

In system (9) a single equation with FPs from two electrodes is sufficient for the solution. If the number of electrodes increases, system (9) expands with additional equations. In a scenario of synchronicity and identical APs, the solutions across all equations in (9) will be identical, which makes the system of equations overdetermined. However, when noise affects the FPs, the solutions may diverge. Despite this divergence, the inherent overdetermined nature of the system can be used to minimize the error introduced by the noise or to select the solution with the best signal-to-noise ratio.

The availability of multiple solutions from different electrodes in (9) also enables a synchronicity test: if the solutions are equal (or sufficiently similar in the presence of noise), then the APs can be considered synchronous.

Figure 6a shows that using equation (9) when there is a delay between the FPs can result in inaccurate reconstruction. In contrast, the equations from (8) effectively compensate for this delay. Figure 6b demonstrates how reconstructing asynchronous APs using (9) alters the APs' waveforms and their duration-related characteristics (including depolarization and repolarization durations, which add up to full AP duration (APD); Fig. 6c shows how APD changes depending on the introduced delay). Consequently, this can influence metrics derived from these characteristics, like AP prolongation and shortening, which are important indicators in cardiotoxicity assessments. AP prolongation, for instance, can be associated with drug-induced QT interval prolongation, a known risk factor for life-threatening arrhythmias like Torsades de Pointes. Accurate evaluation of these metrics is critical for a comprehensive understanding of potential cardiotoxic effects and ensuring patient safety in drug therapies.

Conclusions

This study describes a method to reconstruct cardiac cells' APs based on their FPs in the cases of AP asynchronicity or partial synchronicity. While the synchronicity of FPs can simplify the reconstruction by minimizing the number of unknown AP, the asynchronous behaviour (delay between FPs or different FP frequencies) increases that number. The numerical experiment demonstrated in this paper showed that when AP are identical and synchronous, the system of N equations with N unknown variables transforms into a system of N equations with 1 unknown variable, which allows to determine an AP using FP from any pair of available electrodes. Conversely, when the APs are generated by a group of N cells independently and asynchronously using the reconstruction method designed for synchronous AP behaviour can result in inaccurate reconstruction. Accurately reconstructing APs of cells using their FPs expands the number of characteristics available for cardiotoxicity assessment in MEA systems.

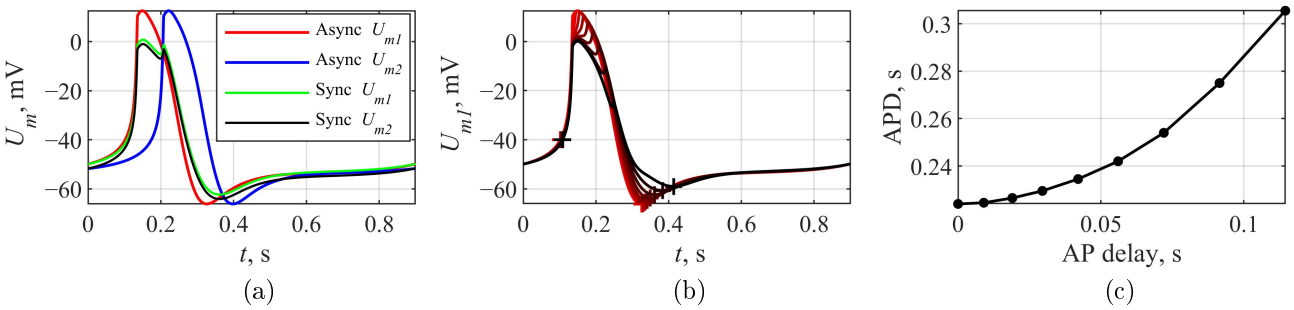

Fig. 6. Simulated APs reconstructed from delayed FPs (a) using formula for asynchronous AP (8) (red and blue APs) and synchronous AP (9) (green and black APs); APs reconstructed using formula for synchronous AP (8) with different time-delayed FPs (b), where red stands for no delay and black for increasing delay; influence of time delay between FPs on reconstructed APs' duration (c)

Acknowledgements

The authors would like to express their gratitude to the researchers at Politecnico di Milano, especially A. Redaelli and R. Visone, for sharing a video of contracting cardiac tissue in the μECG device.

Interests disclosure

The authors have no conflicts of interest to declare.

References

[1] Novellino, A., Scelfo, B., Palosaari, T., et al. (2011). Development of micro-electrode array based tests for neurotoxicity: assessment of interlaboratory reproducibility with neuroactive chemicals. *Frontiers in Neuroengineering*, Vol. 4. DOI: 10.3389/fneng.2011.00004.

[2] Mulder, P., de Korte, T., Dragicevic, E., et al. (2018). Predicting cardiac safety using human induced pluripotent stem cell-derived cardiomyocytes combined with multi-electrode array (MEA) technology: A conference report. *Journal of Pharmacological and Toxicological Methods*, Vol. 91, pp.36-42. DOI: 10.1016/j.vascn.2018.01.003.

[3] Shih, H. T. (1994). Anatomy of the action potential in the heart. *Texas Heart Institute Journal*, Vol. 21, Iss. 1, pp. 30-41.

[4] Boyett, M. R., Honjo, H. and Kodama, I. (2000). The sinoatrial node, a heterogeneous pacemaker structure. *Cardiovascular research*, Vol. 47, Iss. 4, pp. 658-687. DOI: 10.1016/s0008-6363(00)00135-8.

[5] Tertoolen, L. G. J., Braam, S. R., Van Meer, B. J., Passier, R. and Mummery, C. L. (2018). Interpretation of field potentials measured on a multi electrode array in pharmacological toxicity screening on primary and human pluripotent stem cell-derived cardiomyocytes. *Biochemical and Biophysical Research Communications*, Vol. 497, Iss. 4, pp. 1135-1141. DOI: 10.1016/j.bbrc.2017.01.151.

[6] Duan, X., Gao, R., Xie, P., et al. (2012). Intracellular recordings of action potentials by an extracellular nanoscale field-effect transistor. *Nature Nanotechnology*, Vol. 7, Iss. 3, pp.174-179. DOI: 10.1038/nnano.2011.223.

[7] Cerea, A., Caprettini, V., Bruno, G., et al. (2018). Selective intracellular delivery and intracellular recordings combined in MEA biosensors. *Lab on a Chip*, Iss. 22, pp. 3492-3500. DOI: 10.1039/C8LC00435H.

[8] Nick, C., Joshi, R., Schneider, J. J. and Thielemann, C. (2012). Three-Dimensional Carbon Nanotube Electrodes for Extracellular Recording of Cardiac Myocytes. *Biointerphases*, Vol. 7, Iss. 1. DOI: 10.1007/s13758-012-0058-2.

[9] Dipalo, M., Amin, H., Lovato, L., et al. (2017). Intracellular and Extracellular Recording of Spontaneous Action Potentials in Mammalian Neurons and Cardiac Cells with 3D Plasmonic Nanoelectrodes. *Nano letters*, Vol. 17, Iss. 6, pp. 3932-3939. DOI: 10.1021/acs.nanolett.7b01523.

[10] Iachetta, G., Melle, G., Colistra, N., Tantussi, F., De Angelis, F. and Dipalo, M. (2022). Chronic cardiotoxicity assessment by cell optoporation on microelectrode arrays. *bioRxiv*, pp. 2022-06. DOI: 10.1101/2022.06.20.496820.

[11] Jans, D., Callewaert, G., Krylychkina, O., et al. (2017). Action potential-based MEA platform for in vitro screening of drug-induced cardiotoxicity using human iPSCs and rat neonatal myocytes. *Journal of Pharmacological and Toxicological Methods*, Vol. 87, pp. 48-52. DOI: 10.1016/j.vascn.2017.05.003.

[12] Zlochiver, V., Kroboth, S. L., Beal, C. R., Cook, J. A. and Joshi-Mukherjee, R. (2019). Human iPSC-Derived Cardiomyocyte Networks on Multiwell Micro-electrode Arrays for Recurrent Action Potential Recordings. *JoVE (Journal of Visualized Experiments)*, (149), p. e59906. DOI: 10.3791/59906.

[13] Zhang, Z., Zheng, T. and Zhu, R. (2020). Single-cell individualized electroporation with real-time impedance monitoring using a microelectrode array chip. *Microsystems & Nanoengineering*, Vol. 6, Article number: 81. DOI: 10.1038/s41378-020-00196-0.

[14] Davis, A. A., Farrar, M. J., Nishimura, N., Jin, M. M. and Schaffer, C. B. (2013). Optoporation and Genetic Manipulation of Cells Using Femtosecond Laser Pulses. *Biophysical Journal*, Vol. 105, Iss. 4, pp. 862-871. DOI: 10.1016/j.bpj.2013.07.012.

[15] Ivanushkina, N. G., Ivanko, K. O., Shpotak, M. O. and Prokopenko, Y. V. (2022). Reconstruction of Action Potentials of Cardiac Cells from Extracellular Field Potentials. *Radioelectronics and Communications Systems*, Vol. 65, Iss. 7, pp. 354-364. DOI: 10.3103/S0735272722090047.

[16] Visone, R., Ugolini, G. S., Cruz-Moreira, D., et al. (2021). Micro-electrode channel guide (μECG) technology: an online method for continuous electrical recording in a human beating heart-on-chip. *Biofabrication*, Vol. 13, Iss. 3, 035026. DOI: 10.1088/1758-5090/abe4c4.

[17] Shpotak, M., Ivanushkina, N., Ivanko, K. and Prokopenko, Y. (2022). A Model for Simulation of Human Sinoatrial Node Action Potential. *2022 IEEE 41st International Conference on Electronics and Nanotechnology (ELNANO)*, pp. 422-425. DOI: 10.1109/elnano54667.2022.9927001.

[18] Pohl, A., Wachter, A., Hatam, N. and Leonhardt, S. (2016). A computational model of a human single sinoatrial node cell. *Biomedical Physics & Engineering Express*, Vol. 2, Iss. 3, 035006. DOI: 10.1088/2057-1976/2/3/035006.

[19] Visone, R., Talò, G., Occhetta, P., et al. (2018). A microscale biomimetic platform for generation and electromechanical stimulation of 3D cardiac microtissues. *APL Bioengineering*, Vol. 2, Iss. 4. DOI: 10.1063/1.5037968.

Визначення потенціалів дії багатьох клітин серця за потенціалами позаклітинних полів

Шпотак М. О., Іванушкіна Н. Г., Іванько К. О., Прокопенко Ю. В.

В сучасних біомедичних технологіях, системи з мікроелектродними решітками (МЕР) використовують разом з штучно вирощеними клітинами для вивчення біологічних механізмів захворювань і тестування впливу лікарських препаратів. Сучасні МЕР-системи вимірюють позаклітинні потенціали поля (ПП) культур клітин або тканин, але не можуть реєструвати внутрішньоклітинні потенціали дії (ПД) без технологічних модифікацій або додаткових пристроїв, що обмежує глибину аналізу електрофізіології клітин. Одним з можливих рішень проблеми нездатності МЕР-систем вимірювати ПД є їх математична реконструкція із зареєстрованих ПП. Однак точна реконструкція ПД декількох клітин одночасно ускладнюється такими факторами, як кількість клітин, синхронність та відмінність морфології їхніх ПД, ідентифікація їхніх електрофізіологічних параметрів та наявність шумів. Метою цієї статті є врахування синхронності, асинхронності та часткової синхронності ПД клітин в методі реконструкції. Щоб розв'язати поставлену задачу отримано систему рівнянь, здатну реконструювати ПД N клітин одночасно, використовуючи записані з $N+1$ електрода ПП. Система рівнянь враховує кількість клітин, синхронність ПД різних клітин та електричні властивості клітин та середовища. Модельні експерименти реконструкції ПД з ПП проведено для випадків з різними типами синхронності та за наявності шуму. Реконструйовані ПД у поєднанні із записаними ПП розширюють кількість електрофізіологічних характеристик для оцінювання кардіотоксичності в МЕР та інших багатоелектродних пристроях.

Ключові слова: потенціали дії; потенціали поля; реконструкція сигналу; синхронність сигналу; чисельне моделювання; клітинна електрофізіологія; мікроелектродна решітка